CORONAL AND INTERPLANETARY PROPAGATION, INTERPLANETARY ACCELERATION, COSMIC-RAY OBSERVATIONS BY DEEP SPACE NETWORK, AND ANOMALOUS COMPONENT

C. K. Ng

Dept. of Mathematics, University of Malaya
Kuala Lumpur 22-11, Malaysia

1. Introduction

The purpose of this rapporteur paper is to provide an overview of the contributions presented in sessions SH3, SH1.5, SH4.6 and SH4.7 of the 19th International Cosmic Ray Conference. These contributed papers indicate that steady progress continues to be made in both the observational and the theoretical aspects of the transport and acceleration of energetic charged particles in the heliosphere.

Studies of solar and interplanetary particles have placed emphasis on particle directional distributions in relation to pitch-angle scattering and magnetic focusing, on the rigidity and spatial dependence of the mean free path, and on new propagation regimes in the inner and outer heliosphere. Coronal propagation appears in need of correlative multi-spacecraft studies in association with detailed observation of the flare process and coronal magnetic structures. Interplanetary acceleration has now gone into a consolidation phase, with theories being worked out in detail and checked against observation.

With the approach of the solar minimum, and with the Pioneers and the Voyagers spacecraft advancing steadily towards the heliospheric boundary, observation of the galactic cosmic rays and the anomalous component will soon, we hope, help to unravel the mystery of solar modulation (see Kota, 1985).

2. Coronal And Interplanetary Propagation

Flare-associated solar energetic particles (SEP) are usually assumed to have been accelerated at the sun, and to have subsequently propagated through the corona and interplanetary space before being detected. Theories tend to treat these three processes separately, using the result of the preceding stage as input to the subsequent stage.

It is however a complicated task to isolate the effects of the three processes from the observations because of the uncertainty and great variability from event to event in the flare process, and in the conditions of the corona and interplanetary space. In some cases, a large-scale shock is observed to propagate through the corona and interplanetary space. If particles are continuously accelerated by the shock on open field lines, coronal acceleration and propagation may be intrinsically inseparable, and one must also take account of the shock as a moving particle source and reflector in interplanetary space.

2.1 Coronal Propagation

Since the mid-sixties, coronal propagation has been studied by finding the dependence of the observed onset times, rise times, energy spectra and abundance ratios of SEP events on heliographic angular separation from the flare site. The angle dependence is deduced by (a) statistical analysis of single-spacecraft data from many events, or (b) concurrent multi-spacecraft data of individual events. In addition, the

coronal diffusion coefficient $K_\odot$ and coronal escape rate η have been determined for many events, using single-spacecraft data on concurrent intensity and anisotropy time histories.

The statistical studies have established the east-west asymmetry of the onset time and rise time, the existence of the fast propagation region (FPR) at 0°W - 100°W, the variation of event size with angular separation, and the correlation of p/α ratio with event size (see Van Hollebeke, 1979, and references therein). However, conflicting observations of the longitudinal variation of the proton spectra have been reported in both statistical and multi-spacecraft studies, and different conclusions regarding the rigidity and energy dependence/independence of the coronal propagation parameters have been made (see e.g. Mason *et al.*, 1984, and references therein). Nevertheless, it seems clear that the dependence of $K_\odot$ and η on energy and rigidity, if any, is weak. Some evidence seems to indicate that outside the FPR these parameters increase only with particle velocity.

The intensities and p/α ratios of solar particle events observed by the geostationary satellites GMS-1 and 2 from Feb 1978 to Sept 1984 are analysed in papers SH3.1-1 and 2 (unfortunately not presented). Using statistics from 50 events, Takenaka *et al.* (SH3.1-1) confirm the east-west effect in the rise-time and the existence of the FPR. Finding a possible correlation between short-rise time events and the occurrence of an SSC < 8 days before the events, they suggest the folowing interesting scenario. Particles from a western flare propagate rapidly in relatively smooth magnetic fields established behind an interplanetary shock, caused by a preceding eastern flare in the same active region. If confirmed, this would be relevant in interpreting the FPR and the east-west effect.

Kohno *et al.* (SH3.1-2) find that, in 14 out of 16 fast-rise events in the FPR, after adjustment for the Sun-Earth travel times, the protons in 5 energy channels between 8 to 500 MeV have almost identical intensity time profiles (Fig 1). Assuming that these reflect essentially the injection time profiles, the authors infer rigidity and energy independent coronal propagation in the FPR. We note that this appears contrary to the conclusion of Bazilevskaya & Vashenyuk (1979) for > 100 MeV protons. These onset delay times in the FPR bear no relation to angular separations from the flare site and appear consistent with the magnetic bottle model and the large-scale shock acceleration (LSSA) model (see below).

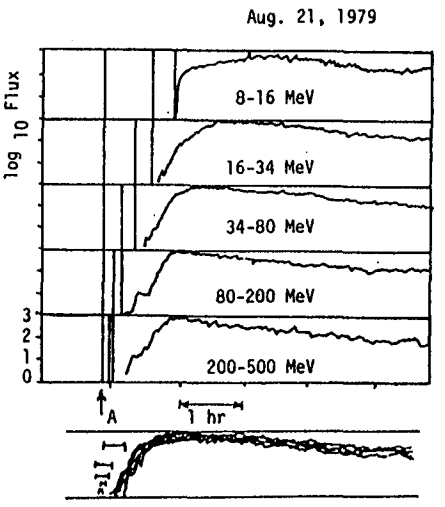

Fig 1

In paper SH3.1-3, Schellert *et al.* report on a statistical study of 36 events observed by Helios 1 and 2. From their plot of the time-to-maximum vs angular separation (Fig 2), they deduce that outside the FPR, for ~0.5 MeV electrons, $t_E t_D$ = 55 h², where t_E

and t_D are the coronal escape time and diffusion time respectively. The difference between this value and $t_E t_D$ = 800 h² for ~10 MeV protons (e.g. McGuire *et al.*, 1983; Ng and Gleeson, 1976), as well as the difference between concurrent proton and electron intensities observed on Helios 1 and 2 (their Fig. 3), show that the electrons propagate faster than the protons in the corona, leading Schellert *et al.* to reject species-independent models like the bird-cage model and the large-scale shock model (see below). From the wide range of the observed angular gradients of the maximum intensity of ~0.5 MeV electrons, apparently unrelated to the FPR (their Fig 2), Schellert *et al.* conclude that there is no universal process for coronal diffusion.

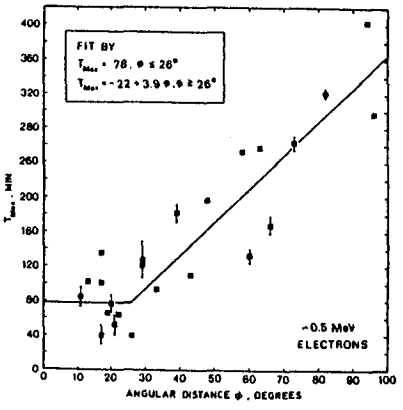

Fig 2

For the 4 Nov 1978 and 20 Nov 1978 events, when Prognoz-7 and Venera-11 were connected to neighbouring points in different unipolar magnetic field regions (UMRs) of the sun, these spacecraft observed an order of magnitude decrease in the fluxes and a large increase (~10 hr) in the rise time of ~5 MeV protons across the UMR boundary (Fig 3 from Morozova *et al.*, paper SH3.1-6, not presented). These authors deduce that the coronal propagation speed is ~ 140°/h in a UMR but drops to only 2 -5°/h across the boundary. We note that the observation may also be qualitatively consistent with the decreased efficiency of particle acceleration by a coronal shock after it has crossed a neutral sheet (Steinolfson and Mullan, 1980). It would be worthwhile to know if the UMR boundary has a similar effect on the electrons.

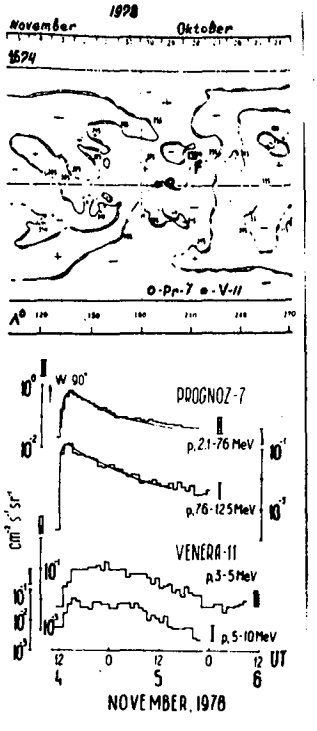

Fig 3

In summary then, the above conference papers have reported general observational confirmation of previous findings on the east-west effect and FPR, a possible correlation between fast-rise particle events and preceding SSC's, strong evidence for rigidity and energy independent injection of 8 - 500 MeV protons from the FPR, the species dependence of large scale coronal transport outside the FPR, and large attenuation in proton intensity time history across UMR boundaries.

To understand the observations, we shall discuss a few theoretical models. The angular dependence of the rise time and the event size outside the FPR can be explained by Reid's (1964) phenomeological model (called CODE model below). It assumes 2-D

particle diffusion in a thin spherical shell of radius a over the sun, with random escape into interplanetary space. The particle differential number density N(X,T,t), at kinetic energy T and heliographic angular separation X from the axis of a symmetric particle source, is governed by

$$\frac{\partial N}{\partial t} = \frac{1}{a^2 \sin X} \frac{\partial}{\partial X}\left(K_S \sin X \frac{\partial N}{\partial X}\right) - \eta N \qquad (1)$$

(Ng and Gleeson, 1976). Here $K_s(T)$ is the coronal diffusion coefficient and $\eta(T)$ the escape rate. It is customary to define the diffusion time $t_D = a^2/K_s$, and the escape time $t_E = 1/\eta$. The solution may be written in the form $N(X,T,t) = N_o(T)\, Q(X,\tau;g)$, where $N_o(T)$ is the source spectrum, and Q is a function which depends on the angle X, the dimensionless time $\tau = t/t_D$, and the dimensionless parameter $g = t_D/t_E$. For given X and T, Q and hence N attain maximum at $\tau = \tau_{max}(X;g)$, and $N_{max}(X,T) = N_o(T) Q[X,\tau_{max}(X;g);g]$.

The maximum injection rate into interplanetary space is $I_{max} = \eta N_{max}$, and its spectrum is given by

$$\frac{\partial \ln I_{max}}{\partial \ln T} = \frac{d \ln N_o}{d \ln T} + \frac{d \ln \eta}{d \ln T} - \tau_{max}(X;g)\, T \frac{dg}{dT} \quad . \qquad (2)$$

This equation is relevant for the interpretation of observations in terms of the CODE model. First, the injection spectrum at maximum may be modified from the source spectrum by an energy-dependent escape rate $\eta(T)$. Secondly, since $\tau_{max}(X;g)$ clearly increases with X, the spectrum softens with increasing X if and only if $dg/dT > 0$, i.e. t_D/t_E increases with increasing energy. This also means that the independence of the spectral index and p/∝ ratio on X do not in themselves imply rigidity-independent t_D and t_E. The conclusion only follows if one further establishes by *independent means* the rigidity independence of either t_D or t_E. For planar approximation and a point source,

$$Q(X,\tau;g) = (1/4\pi\tau)\, \exp\,(-X^2/4\tau \; - g\tau) \qquad (3)$$

(Reid, 1964). A spherical solution for a spatially extended source is given in Ng and Gleeson (1976).

The CODE model leaves the mechanism of coronal diffusion and escape unspecified. In Newkirk and Wentzel's (1978) 'bird-cage' model, particles are transported from magnetic loops to magnetic loops via field-line reconnection produced by the rearrangement of the field in the supergranulation network, resulting in rigidity and energy-independent K_s and η for < 40 MeV protons and < 80 MeV electrons.

In Mullan and Schatten's (1979) two-component model, (a) rigidity and energy independent transport in the FPR is due to the breaking of an expanding magnetic bottle ~ 15 min after a flare and (b) outside the FPR (X > 60°), the particles are scattered by magnetic inhomogeneities with scale sizes > 500 km, resulting in a coronal diffusion coefficient dependent on particle velocity but independent of particle mass. The particles also experience mainly east-west gradient and curvature drifts in the mainly north-south oriented large scale coronal loops.

In yet another model (LSSA model), suggested by Lin and Hudson (1976) and favored in a number of recent works (e.g. Mason *et al.*, 1984 , and references therein), a rapidly expanding (~ 1000 km/s) large-scale coronal shock accelerates particle on open field lines which lead directly into interplanetary space, thus obliterating the distinction

between coronal acceleration, propagation and escape.

As concluded in paper SH3.1-2, the magnetic bottle and LSSA models both appear consistent with the observed rigidity and energy independent particle injection from the FPR. It is possible that after breaking the bottle, the shock continues to accelerate particles on open field lines. However, according to Mason *et al.* (1984), the magnetic bottle model is inconsistent with the observed independence of abundance ratios (at ~ 1 MeV/nuc) on ionization loss in the corona.

Outside the FPR, the difference between the coronal transport of protons and electrons appears to support the two-component model (i.e. the CODE model). However, an *angle dependent* LSSA model may yet be consistent with this observation.

We must also point out here the important implication of the existence of two classes of flares demonstrated by Cane *et al.* in a different session (SH1.2-12). Class I flares are compact and occur low in the corona. Class II flares are diffuse, occur higher in the corona, and tend to be associated with coronal mass ejections. Whilst both classes of flares produce comparable electron events, Class I flares tend to produce far smaller proton events than Class II flares.

This suggests that coronal acceleration and transport depend on the altitude and the nature of the flare, and that more than one model of coronal acceleration/transport may be necessary. If so, the SEP data of Class I and Class II flares should be analysed separately for the effects of coronal acceleration/storage/transport.

From the above discussion, we see that progress has been made and it is hoped that a consistent picture of coronal transport will emerge in the near future. To this end, we need good angular and temporal resolution, that is, as complete as possible a set of *concurrent multi-spacecraft* data, including SEP directional intensities, spectra and composition, plasma flow (for mapping back to the corona), interplanetary and coronal magnetic fields, solar optical, radio, X and γ-ray emissions.

More theoretical work is also required. A clear quantitative difference between the predictions of the CODE model and the LSSA model is important for deciding between diffusive transport or shock acceleration outside the FPR. As the shock parameters (e.g. field-normal angle) should depend on heliographic angular separation, this fact should be taken into account in a quantitative LSSA model.

2.2 Interplanetary Propagation

After escaping from the corona to the solar-wind medium, solar energetic charged particles are guided and focused by the large-scale interplanetary magnetic field (IMF) and scattered by small-scale magnetic irregularities. Because of the large and small-scale electric fields induced by the motion of the IMF and magnetic irregularities, the particles also experience the $\underline{E}x\underline{B}$ drift, adiabatic deceleration and second order Fermi acceleration. The particles may also be reflected or transmitted at interplanetary shocks and experience energy changes during shock encounter.

In this section, we shall group the conference papers around the following headings and discuss them in that order: (a) interplanetary mean free path, (b) directional particle distributions, and (c) new propagation regimes.

2.2.1 Interplanetary Mean Free Path

In papers SH3.2-5, 3.1-8A and 3.2-9, the model of diffusion, convection and adiabatic deceleration (DCA model) is used to find the spatial and rigidity dependence of the radial mean free path λ_r from SEP events.

During the much studied 22 Nov 1977 event, Voyagers 1 and 2 at $\sim$ 1.5 AU and the earth are all well-connected to the flare site. Assuming an injection $\propto \exp(-t/\sigma)$ and a radial diffusion coefficient $K=K_o r^b$, Mason *et al.* (SH3.2-5) fit simultaneously the 0.6 -1 MeV/nuc helium intensities measured on ISEE 1 and Voyager 2, with the parameters σ = 12 ± 3 hrs, b = 1.3 ± 0.1 and λ_r = 0.10 ± 0.02 AU at 1 AU. Assuming rigidity-dependent $K_o \propto (A/Z)^{0.88}$, the intensity histories of 0.6 - 1 MeV/nuc H, C, O, and Fe are calculated (Fig 4). Except for proton (lowest rigidity) at both spacecraft and Fe (highest rigidity) at Voyager 2, all intensity fits are satisfactory. Mason *et al.* suggest rigidity-dependent interplanetary acceleration as the cause of the discrepancy.

For the same event, Hamilton *et al.* (SH3.1-8) consider not only the intensities of 1 and 25 MeV/nuc protons and helium at 1 AU and 1.6 AU, but also their anisotropies at 1.6 AU. They find $\lambda_r \sim$ 0.1 AU at 1 AU also, but have to abandon the simple power-law radial dependence of K_r in an attempt to fit all the observations.

In paper SH3.2-9 (not presented), Chebakova *et al.* fit the intensities of protons, helium and electrons of various energies in the 28 May 1967 and 2 Nov 1969 events. Assuming impulsive solar injection and $K_r \propto r^{b(R)} R^{\alpha}$, they find α = 0.27 and 0.6 for the two events and b increasing with rigidity R, thus concluding that $K_r(r,R)$ is not separable in r and R.

This conclusion, based on the assumption of impulsive injection, should be contrasted with the approach in paper SH3.2-5, in which b is assumed constant, but the injection is non-impulsive. The three papers above illustrate the difficulty of separating the effects of solar injection, interplanetary acceleration and interplanetary propagation. They underscore the importance of multi-spacecraft data and anistropy measurements, which together require fewer assumptions in the model.

In paper SH3.2-6, Lockwood and Debrunner extend previous analysis of the May 7, 1978 event at 1 AU to the observation of 70 - 500 MeV protons of the same event

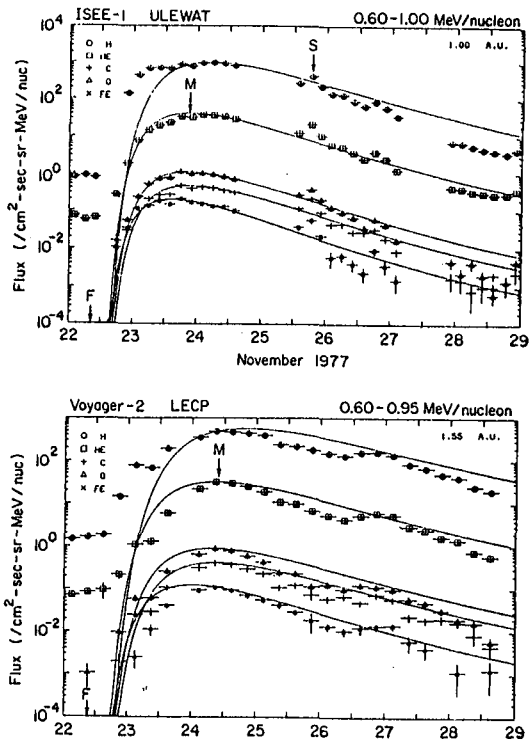

Fig 4

observed at Voyagers 1 and 2 at ~ 3 AU. They adopt (a) the Reid-Axford injection with $K_{\theta}\,[cm^2/s] = 4.4 \times 10^{18}\,(E\,[MeV])^{1/2}$ and $\eta = (2.9 + 0.5)\ hr^{-1}$, and (b) scatter-free propagation at $r < 1.6$ AU and diffusive propagation beyond. They deduce that $\lambda = 0.04$ AU beyond 1.6 AU. However, the model of coronal injection appears inconsistent with the observation at Helios A, and further studies with a more refined interplanetary transport model would be worthwhile.

In paper SH3.2-11, Lumme *et al.* fit the intensity and anisotropy of the May 7, 1978 ground level event (GLE) by a Monte Carlo simulation which takes into account adiabatic focusing, isotropic pitch-angle scattering and an injection $\propto \exp(-t/\sigma)$. They obtain $\lambda = 1$ AU and $\sigma = 11$ min, in contrast to $\lambda = 3 - 5$ AU reported in Lockwood *et al.* (1982).

The cause of the big difference is not completely clear. We note however the following. (a) The anisotropy observed by Lumme *et al.* decays somewhat faster than that observed by Lockwood *et al.* (b) The injection functions are not very different. (c) For $\lambda = 1$ AU, the theoretical anisotropy profile of Lockwood *et al.* (their Fig 5) decays significantly faster than that of Lumme *et al.* (their Fig 4). (d) Both groups simulate the distance between collisions with an exponential probability distribution: $(1/\lambda)\exp(-\Delta s/\lambda)$. However, whereas Δs is the distance projected along the field line in Lumme *et al.*, it is the actual distance in Lockwood *et al.*

Factors (a) and (d) both tend to yield a smaller value of λ for Lumme *et al.* Note that the adopted exponential distribution is very broad with 39% and 13.5% probability that $\Delta s < \lambda/2$ and $\Delta s > 2\lambda$ respectively. A probability distribution of a much smaller range would be more realistic. Since a particle travelling sunward will mirror even in the absence of scattering, the effective mean free path would be smaller than the value of λ used in the simulation.

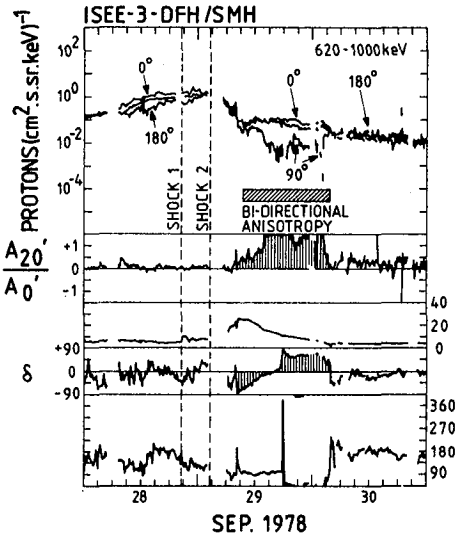

Fig 5

2.2.2 Directional Particle Distributions

With improving instrumental resolution and theoretical advance, there has been increasing interest in the directional distribution of solar energetic particles. In paper SH3.1-9, Marsden *et al.* report on a most comprehensive survey of 66 periods (> 3 hr each) of bidirectional anisotropies observed on ISEE-3 during Aug 1978 - May 1982. Fig 5 shows the bidirectional flow (BDF) event of 29 Sept 1978. They have classified and analysed the events according to magnetic field signatures and association with interplanetary shocks. They conclude that the simple model of a large-scale magnetic loop anchored on the sun cannot explain all the BDF events, and that localised effects cannot be ruled out. They also emphasise the qualitative correlation between the quietness in the

magnetic field magnitude and BDF event occurrence.

The description of a directional distribution depends on the choice of a reference frame. Transformation from the spacecraft frame to a chosen comoving frame is almost always necessary for the interpretation of the directional distribution of low-energy ions. For > 10 KeV protons, the hitherto complicated transformation procedures are rendered unnecessary by a set of second-order correct explicit transformation formulae presented by Ng in paper SH3.1-10. These are of the form

$$A_{nm}(p) = \text{function}\left\{ A^{sc}_{jk}(p),\ \partial A^{sc}_{jk}/\partial p,\ \partial^2 A^{sc}_{jk}/\partial p^2 \right\} + O(W/v)^3,$$

where A_{nm} and A^{sc}_{jk} are the spherical harmonic coefficients in the comoving frame and the spacecraft frame respectively, W the transformation velocity, v the particle velocity, and p the momentum.

In SH3.1-11, Ng describes a method to determine the particle directional distribution (in terms of pitch-angle and gyrophase), the harmonic anisotropies and associated Poisson errors from sectored particle data and concurrent field and plasma flow direction.

A concise and effective format is used to present directional solar particle data in Fig. 2 of SH3.1-11, for the 1.4 - 2.5 MeV protons of the Day 118, 1978 event observed on IMP-8. In this event, as the IMF direction varies, the variation in the transverse anisotropy in the ExB drift direction is in phase with but far larger than the variations in the Compton-Getting anisotropy. Magnetic connection to the bow shock does not appear to explain all the variations. Further work is necessary to find out the cause of this behavior.

Attempts to determine and interpret the pitch-angle distribution of the 16 Feb 1984 GLE event are reported in papers SH3.1-7, SH3.2-1 and SH3.2-2. Analysing the first two five-minute data from various stations, Fenton *et al.* (SH3.2-2) find no satisfactory mean arrival direction consistent with the asymptotic directions of the stations. On the other hand, Debrunner *et al.* (SH3.1-2) deduce the mean direction at 5°S, 5°E geographic coordinates. IMF data from ICE (ISEE-3) would be helpful in this regard.

Using the CODE model, Debrunner *et al.* calculate the intensity time profiles assuming two possible flare sites at 95°W and 130°W, and decide for 95°W upon comparison with the observation. The pitch-angle distribution observed at the time of maximum intensity (their Fig 3) is much narrower than the hourly average distribution (Fig. 6) deduced in paper SH3.2-1. This suggests that the distribution did broaden significantly in the first hour.

In paper SH3.2-13, Niskovskikh and Filipov analyse 5 GLEs associated with preceding propagating interplanetary shocks and 4 GLEs associated with preceding CIRs. They conclude that the onset delay between different stations and the ocassional second hump in the intensity are caused by

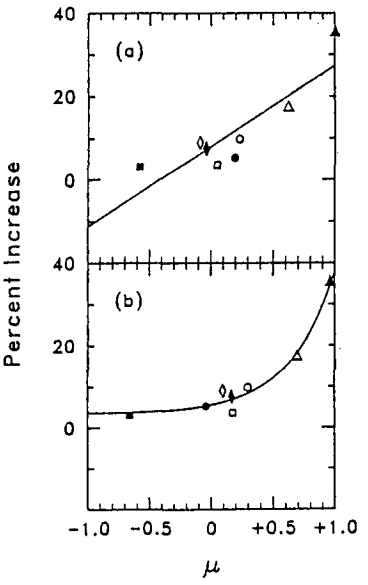

Fig 6

scatter-free propagation, partial reflection at the shock and particle mirroring near the sun.

The new idea of determining local interplanetary scattering parameters *directly* from the observation of particle pitch-angle distribution underlies the studies reported in three papers, SH3.1-13A, SH3.2-8A and SH3.2-1. This approach simplifies the hitherto involved procedure used in the fitting of the pitch-angle distributions of SEP events (e.g. Ng *et al.*, 1983). Beeck and Wibberenz (SH3.1-13A) exploit the properties of an approximate solution of the focused transport equation to deduce the pitch diffusion coefficient $k(\mu)$ directly for a number of events with λ ranging from 0.1 to 1 AU. Using a code from Ng to solve numerically the focused transport equation, Green and Schlüter (SH3.2-8A) show that the normalised anisotropic part of the pitch-angle distribution approaches quickly a characteristic function determined only by the local $k(\mu)$ and L. They also show from observations some examples that exhibit the above behaviour. In paper SH3.2-1, Bieber *et al.* assume a pitch-angle distribution of the steady-state form

$$f = C_0 + C_1 B \exp\left\{ (4-q)\,\lambda\mu\,|\mu|^{1-q}/3L \right\},$$

where μ = pitch cosine, B = magnetic field, L = magnetic scale length, λ = mean free path, and C_0, C_1, and q are constant parameters. Fitting this to the observed distributions in the 16 Feb 1984 event yields λ/L = 2 - 10 AU for > 400 MeV protons detected by neutron monitors (Fig 6), and λ/L = 2.8 and q = 1.2 for 35 -145 MeV protons observed on ISEE-3.

A number of papers are concerned with accurate solution of the transport equation in either the DCA model or the focused transport model. In paper SH3.2-10, Yang and Zhang present a method to obtain numerically accurate solution to the DCA model with λ_r = constant. In paper SH4.1-2, Earl derives a general expression of the dispersion coefficient in the theory of focused transport, for λ and L constant. This expression is relevant to an accurate numerical solution of the focused transport equation, as discussed in detail by Earl and Jokipii (SH4.1-3) and Earl (SH4.1-4).

2.2.3 New Propagation Regimes

The highly structured nature of the interplanetary medium and its influence on solar particle propagation are investigated in papers SH3.2-3 for the inner heliosphere and SH3.2-4 for the outer heliosphere. Anderson and Dougherty (SH3.2-3) identify about 50 interplanetary filaments in 1978 and 1979 mainly on the basis of 2 - 10 KeV electron intensities measured on ISEE 3, and further characterise them using concurrent plasma and field data. They find that the filaments have width of .025 ± .015 AU at 1 AU, come in clusters separated by a few hours, trace back to distinctly different regions in the solar corona than surrounding field lines, and

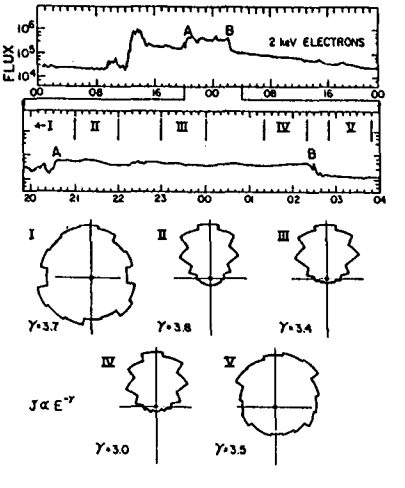

Fig 7

may exhibit decreases or increases in particle intensity relative to the surroundings. The 2 KeV electron angular distribution inside a filament often differs greatly from those outside it (Fig 7). Clearly, the existence of these filamentary channels has important implications for interplanetary propagation.

In paper SH3.2-4A, McDonald and Burlaga report on six SEP events observed between 5 and 12 AU by Pioneer 11, Voyager 1 and Voyager 2. These events are characterised by long time scales ($\sim$1 month), flat energy spectra extending to > 100 MeV and steepening with distance, and association with enhancements of MeV electrons. The authors stress that the outer heliosphere is dominated by systems of interplanetary flows, and the compressive merged interaction regions would have lower diffusion coefficient and lower adiabatic deceleration (Burlaga *et al.*, 1983).

3. Interplanetary Acceleration

Particles may be accelerated in interplanetary space by turbulent magnetic fields (second-order Fermi or statistical acceleration) and also by shocks. In an oblique fast mode shock, particles gain energy in two ways, as seen in the shock frame. (a) Shock drift acceleration (SDA) - particles gain energy by drifting in the direction of the electric field whilst gyrating back and forth across the shock. (b) Diffusive shock acceleration - particles gain energy between scatterings by the converging upstream and downstream magnetic irregularities, and also between scattering upstream and reflection at the shock front (first-order Fermi acceleration).

3.1 Numerical Simulation

There are five papers in which numerical particle trajectory-tracing technique is used to simulate second-order Fermi acceleration and shock acceleration in the presence or absence of waves.

In paper SH1.5-2 (not in the proceedings) Moussas, Valdes-Galicia and Quenby first construct a 'layer model' of the interplanetary magnetic and electric fields, using high resolution plasma and field data from Pioneer 11 at 2.5 AU, during the passage of a CIR on Day 284, 1973. Then, by following test particles in the layer model in the solar wind frame, they find, for 10 - 50 MeV protons, energy loss ahead of the forward shock where grad B is negative, and energy gain in the trailing edge of the CIR where grad B is positive. They also find a statistical energy diffusion coefficient D_{TT} ten times smaller than required to accelerate locally the anomalous component.

Using the same technique, Valdes-Galicia *et al.* (SH1.5-1) find, for a perpendicular shock observed by Helios at 0.45 AU, that there is a three-fold increase in the average energy gain of 100 MeV protons for shock plus statistical acceleration as opposed to shock acceleration only.

By using observed directional particle and field data, and following the particles backward in time, both Kessel *et al.* (SH1.5-5) and Balogh and Erdös (SH1.5-6) carry out consistency checks on the adiabatic theory of single-shock encounter. They find general qualitative agreement between theory and observation. Balogh and Erdös suggest that the model should include fluctuations in Θ_{BN}.

Decker and Vlahos (SH1.5-3) superpose wave fluctuations in an otherwise 60° oblique shock and find that in $\sim$1 hour, 10 KeV protons can be accelerated to yield a spectrum extending to 1 MeV (Fig 8). They also

conclude that the particles gain most of their energy through drift, with scattering merely returning the particles to the shock for more acceleration.

In this context, we note that in the diffusive shock acceleration theory, drift effects are included by Jokipii (1982) and reflection effects are further included by Webb (1983). Nevertheless, for nearly perpendicular shock and/or highly anisotropic particle distributions, diffusion theory may not apply and numerical simulation remains the only available tool.

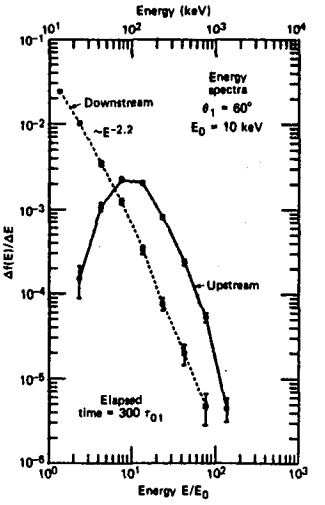

Fig 8

3.2 Observations

The pitch-angle distributions upstream and downstream of five quasi-perpendicular interplanetary shock events (Fig 9) are presented by Balogh and Erdös (SH1.5-6). As stated earlier, they find qualitative agreement with SDA theory but suggest inclusion of fluctuations of θ_{BN} in the model. They also suggest that the double loss cones observed at the higher energies in some events are due to short-lived magnetic bottles intersecting the shocks.

In paper SH1.5-4, Krimigis and Sarris present the ion spectra and the highest time resolution ($\sim$1.2s) counting rates of proton and electrons observed by Voyager 2 in the Jan 6, 1978 shock event, with θ_{BN} = 87.5° and M_A = 3.4 (Fig 10). The enhancements and fine structures down to the scale of a proton gyroradius in the near absence of field fluctuation fit the SDA theory for a quasi-perpendicular shock. A comparison between this shock event and the classic Nov 12, 1978 quasi-parallel shock event shows that in both events, the particle energy density exceeds the field energy density by a factor of 3 to 5 and is a substantial fraction of the shock energy.

Krimigis and Sarris argue that the above and other quasi-perpendicular shock events indicate that SDA at quasi-perpendicular shocks is responsible for accelerating particles to high energies in the interplanetary medium and in the astrophysical context. We refer the reader to Scholer's

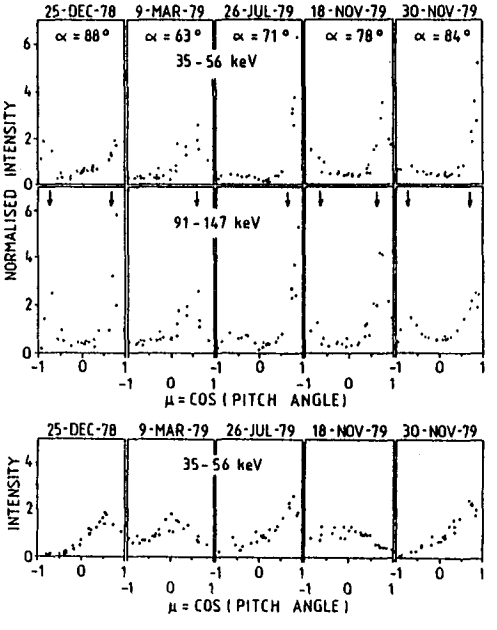

Fig 9

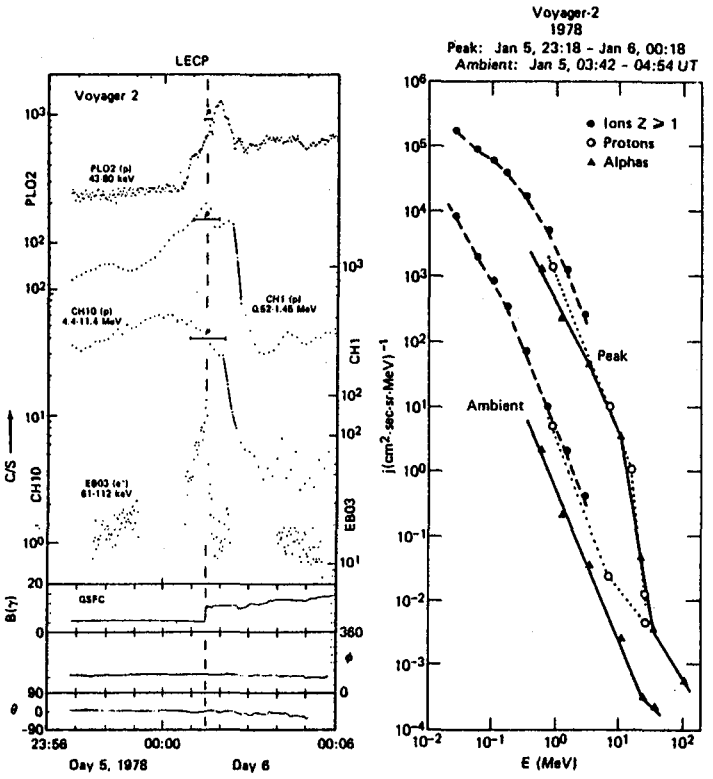

Fig 10

highlight talk at this conference for another view.

With respect to the observation, we note the following. In a single shock encounter, SDA can at most raise the particle energy by a factor of ~ 14 (Decker, 1983). Hence it appears that either the seed particles are of relatively high energies, which raises the question of their origin, or the particles must have encountered the shock many times, which implies scattering. We also note that in this case, the spacecraft is unable to measure field fluctuation in a direction parallel to the field.

In paper SH1.5-12, Gloeckler *et al.* use a novel technique to determine the parallel diffusion coefficient $K_{||}$ upstream of an interplanetary shock. By finding the frame in which the particle distribution is isotropic and thereby the diffusive flux in the spacecraft frame, they find $K_{||}$ as in Fig 11 for the 12 Nov 1978 event. The exponential rise with increasing distance is in accord with Lee's (1983) theory. However, the cause of the slower exponential decrease beyond 5×10^{10} cm is at present unknown.

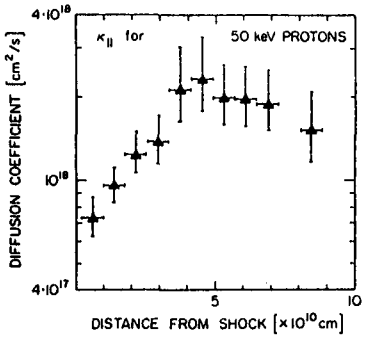

Fig 11

We now turn to shock acceleration

associated with CIRs. Gold *et al.* (SH1.5-14), taking advantage of the latitudinal separation between Voyagers 1 and 2, and picking a period free from solar particle events, show that both the number and the intensity of low energy ion enhancements associated with CIRs in the outer heliosphere (> 12 AU) are smaller at 20°N than at 0° latitude, in agreement with Christon and Stone (1985). However from the similar spectra observed, they conclude that the same acceleration process is at work at both latitudes.

One way to determine the source or the origin of the accelerated particles is to examine their composition. By carefully identifying on ISEE-3 eight CIR-associated events (including the requirement of an easterly anisotropy) in 1984/85, von Rosenvinge and McGuire (SH1.5-15) find H/He = 20 ± 8 at 4.5 - 6.5 MeV/nuc and C/O = .8 ± .2 at 1.8 - 2.8 MeV/nuc, similar to the ratios obtained in 1973/74. These ratios suggest that these particles are accelerated out of the solar wind. However they also find H/He = 67 ± 4 in the 1 Aug 1979 corotating event, and this is consistent with flare particle composition instead. They suggest that for this event, the associated high speed stream was enriched with flare particles injected by known large flares in the previous two solar rotations.

A similar idea is reached independently by Armstrong *et al.* (SH1.5-16). They select a solar active period and a solar minimum period during 1974 - 1981, and classify each day as a flare day, a quiet day, or a non-flare non-quiet day. For the solar minimum period, they find the H/He and He/CNO ratios at 2 - 4 MeV/nuc are distinctly different for the three categories of days. In contrast, in the solar active period, the composition ratios for non-flare non-quiet days are almost identical to the ratios for flare days. They suggest the latter to be due to particles of flare origin.

In paper SH1.5-17 (not presented), Petukhov *et al.* fit the quiet-time spectrum and radial gradients of < 10 MeV proton observed at 1 AU with a model of particle acceleration at the solar wind termination shock. Assuming the shock at 50 AU and reasonable parameter values, they obtain radial gradients of ~10 %/AU at 10 KeV and 5 %/AU at 1 - 10 MeV and a spectrum cut off at ~10 MeV in fair agreement with the observation.

4. Jovian Electrons

Observations of Jovian electron spectrum near Jupiter and at 1 AU are reported by Christon *et al.* (SH1.5-18) and Evenson *et al.* (SH1.5-19) respectively. Fig 12, from SH1.5-19 shows the daily rate of 10 MeV electrons observed by ISEE-3 during 1978 -1984. Apart from the ups and downs associated with the Jovian electron seasons, there is no obvious sign of solar modulation. This and the constancy of the spectrum over 6 years, indicate that solar modulation of electrons at these energies must occur well beyond the orbit of Jupiter. This is consistent with the conclusion that the bulk of the cosmic-ray modulation occur in the distant heliosphere (see below).

A comparison between the 1 AU spectrum and the spectrum measured near Jupiter by Voyagers shows that the 1 AU spectrum bends over below 10 MeV. If real, this may be an effect of rigidity-dependent propagation and adiabatic deceleration.

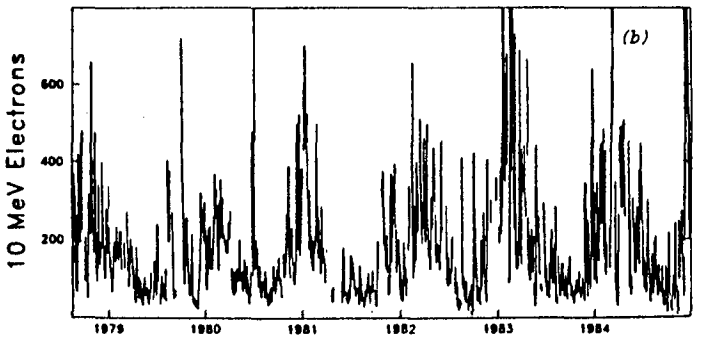

Fig 12

5. Outer Heliosphere, Radial Gradients And Anomalous Component

The network of deep space probes formed by Pioneers 10, 11 and Voyagers 1, 2 together with other spacecraft in the inner heliosphere represents a continuing *in-situ* experiment of the largest (and still expanding) distance scale ever attempted by mankind. Observation by this vast network on the spatial and time dependence of cosmic rays is important for an understanding of the solar modulation process (see Kota, 1985). For this reason, reports of the latest measurements made by this network have been looked forward to at this international cosmic ray conference, just as previous reports had been at past ICRCs. However, the reported gradients are not all in agreement.

Figure 13 (from paper SH4.7-3) shows the heliocentric distances and latitudes of the deep space probes. The wide radial and latitudinal separation between these spacecraft should be kept in mind when one compares their observations and interpretes gradient measurements.

5.1 Cosmic-Ray Intensity in the Outer Heliosphere

Time histories of the cosmic-ray intensities measured by various detectors on the deep space probes over many years are presented in papers SH4.7-1, 2, 3, 5, 6, 7, and 9. An example is given in Fig 14 (from SH4.7-3), which shows the normalised 26-day average proton and helium intensities/rates measured at five spacecraft.

By comparing the intensities at various energies < 500 MeV/nuc measured by Pioneer 10 at 24 - 28 AU in 1981 - 1982 with those measured at 1 AU during the solar minimum in 1977, McDonald *et al.* (SH4.7-3) conclude that the bulk of the modulation of these particles must occur in the distant heliosphere at that time. McKibben *et al.* (SH4.7-5), by comparing the

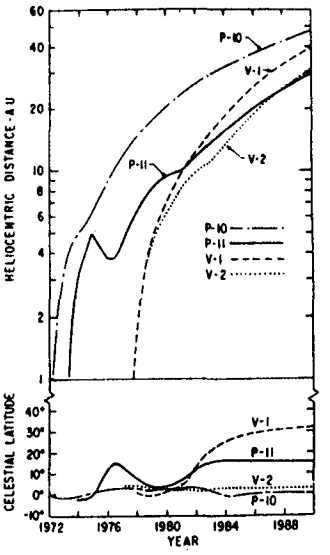

Fig 13

30 - 70 MeV/nuc proton and helium intensities at Pioneer 10 with the estimated interstellar intensities of Evensen *et al.* (1983), conclude that 95% of the modulation of these particles occurred beyond 34 AU in 1984. Similarly, Webber and Lockwood (SH4.7-1) conclude that during 1981 - 1982 about 85% of the modulation of > 60 MeV/nuc cosmic rays must occur beyond 30 AU.

By the end of 1984, the UCSD C1 counting rate of > 500 MeV/nuc ions on Pioneer 10 (SH4.7-2) had recovered to ~80% of its high level in 1978. In contrast, the 121 - 227 MeV proton flux in Fig 14 and the 30 - 57 MeV proton flux (Fig 3 of SH4.7-3) had recovered only to ~40% and ~15% of their 1978 levels. This decreasing level of recovery with lower energy or rigidity (i.e. the hysteresis effect) is true of helium as well. However, in paper SH4.7-4A, Christon *et al.* report that by early 1985, the > 50 MeV electron intensities measured on Voyagers 1 and 2 at 16 AU and 22 AU respectively had recovered to the solar minimum value in 1977, even though the b> 75 MeV proton intensity had only recovered by ~ 80%.

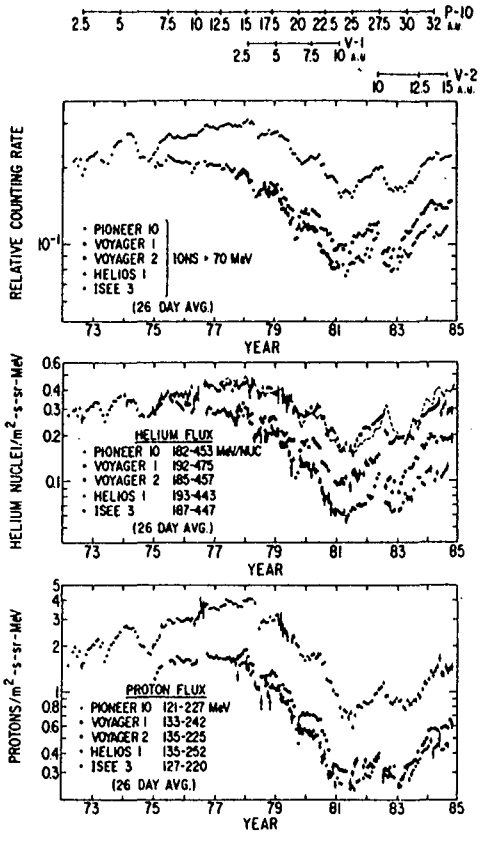

Fig 14

The outward propagation at 400-500 km/s of the step-like decreases of the particle fluxes since 1978 to the minimum level has been previously reported in the literature. In paper SH4.7-7, McKibben *et al.* use the observations of relativistic protons and 30-70 MeV/nuc ions from IMP-8 and Pioneer 10 during 1980-1984 to show that individual *increases* propagated outward at ~ 400 km/s too. However, near the time of the cosmic-ray minimum in 1982 - 1983, the intensity changes, which were not dominated by single events, propagated at ~ 800 km/s.

Forman *et al.* in paper SH4.1-12 (of a different session), show heuristically with a quasi-steady force-field model and numerically with a 3-D time-dependent model, that the phase of solar modulation propagates outward at twice and 1.85 times the solar wind speed respectively. This is caused by the solar cycle variation in the number of scattering barriers between the observer and the modulation boundary, as a result of a change in the frequency of solar emission of such barriers.

The large scale modulation and recovery associated with the huge Forbush decreases observed by Pioneers 10 and 11 in mid-1982 are analysed in paper SH4.7-9 by Pyle and Simpson, using 200-1000 MeV/nuc CNO-Fe counting rates to minimise hysteresis effect. They conclude that these intensity increases and decreases propagated radially outward at

~ 500 km/s and that azimuthal effect is small compared with radial effects.

5.2 Spatial Gradients

Measurements of radial gradients G_r are reported in papers SH4.7-1 to 6 and SH4.6-4 from various experiments aboard the spacecraft. All these (average) gradients have been calculated after time-shifting the data between the two spacecraft at a speed of 400 - 500 km/s, in order to minimise the effect of the outward propagation of modulation.

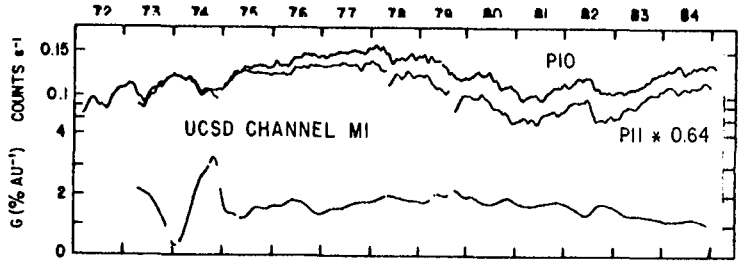

Fig 15

5.2.1 Relativistic Cosmic Rays

Figure 15, from paper SH4.7-2 by Fillius *et al.*, shows the time history of the radial gradient G_r between Pioneers 10 and 11 as measured in the M1 channels (> 80 MeV/nuc) of the UCSD detectors. It shows that since 1982, whilst the intensity has been rising, G_r between the two outermost spacecraft has been decreasing with time. This decreasing trend since 1982 is also reported for G_r measured at smaller distances by Venkatesan *et al.* (SH4.7-6) and Webber and Lockwood (SH4.7-1), but not by McKibben *et al.* (SH4.7-5). Webber and Lockwood report that G_r between IMP 8 and Pioneer 10 decreased from ~ 2.8%/AU in early 1982 to ~ 1.8%/AU in late 1984 (see also Fig 16). In contrast, McKibben *et al.* find that G_r between the same spacecraft remained nearly constant at ~ 2.5%/AU during 1978 -1984.

Figure 16 shows the radial dependence of > 60 MeV/nuc ions measured on IMP-8, Voyagers 1 and 2 and Pioneer 10 at six selected epochs, as reported in SH4.7-1. Note that in Fig 16, G_r remained independent of distance through intensity changes and even after G_r decreased in time. In contrast, Venkatesan *et al.* find that G_r was generally larger between IMP-8 and Voyager 2 than between Voyager 1 and Voyager 2.

Figure 17 summarises the various measurements reported in early 1981 and late 1984. In early 1981, the data would be consistent if the lines join to form a polygon, since Voyager 1 and Pioneer 11 were then close in radius. In late 1984, Pioneer 11 was between Voyager 1 and

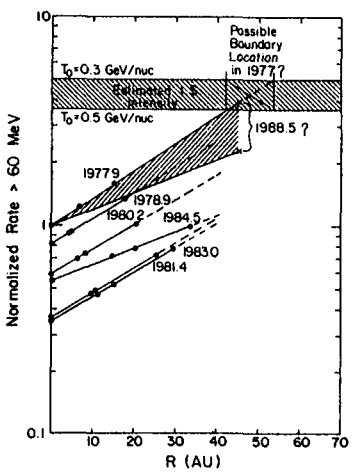

Fig 16

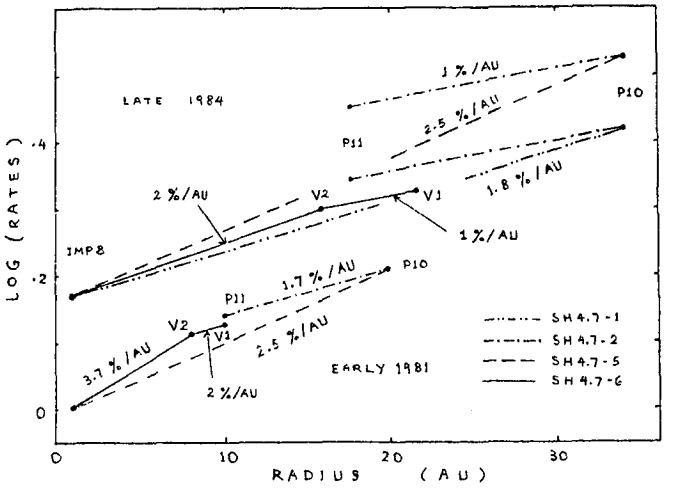

Fig 17

Voyager 2 in both latitude and radius, so the data would be consistent if the line IMP8 - P10 - P11 puts P11 close to the segment V2 - V1 on the line IMP8 -V2 - V1. The data appear consistent for early 1981 but they are inconsistent for late 1984. A (non-unique) way to remove the inconsistency is to adopt G_r somewhat less than 1.8 %/AU between IMP8 and Pioneer 10. One *might* infer that G_r between 1 AU and 20 AU decreased from $\sim$ 2.5 %/AU to $\sim$ 2 %/AU between early 1981 and late 1984, and that for both epochs, G_r decreased with heliocentric distance. However, these inferences must be regarded as controversial at the present time.

The resolution of the discrepancies in the reported spatial and time dependence of G_r probably must await the difficult task of the intercalibration of the various instruments aboard these spacecraft by the various experimental groups. Considering the immense value of the data from the deep space network, such a task may well be worthwhile.

5.2.2 Non-Relativistic Cosmic Rays

Radial gradients of proton and helium of energies < 500 MeV/nuc are reportd by McDonald *et al.* and Mckibben *et al.* Figure 18 from McKibben

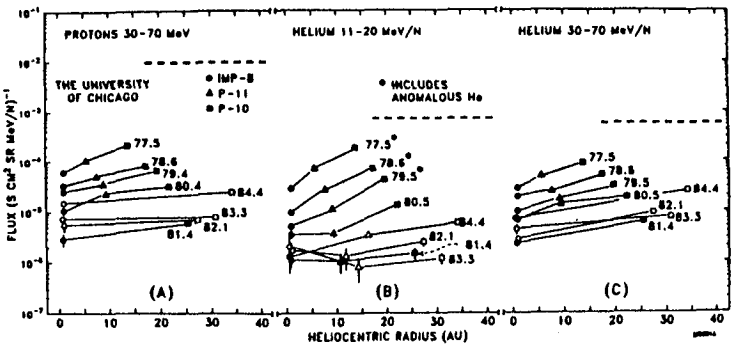

Fig 18

et al. gives yearly snapshots of the intensity versus radius for 30 -70 MeV/nuc protons and helium and 11 - 20 MeV/nuc helium. The radial gradients of these particles were much smaller at and after maximum modulation (1981) than at solar minimum (1977).

Figure 19 from McDonald *et al.* shows, at selected epochs, the radial gradients of proton and helium at various energies in the 'inner' and 'outer' heliosphere. The < 500 MeV protons generally had larger radial gradients than relativistic protons (cf. Fig 15). At solar minimum (1977), all these gradients were significantly larger inside than outside 5 AU. With the onset of solar activity, however, the spatial dependence of G_r changed in a complex manner depending on particle species and energy.

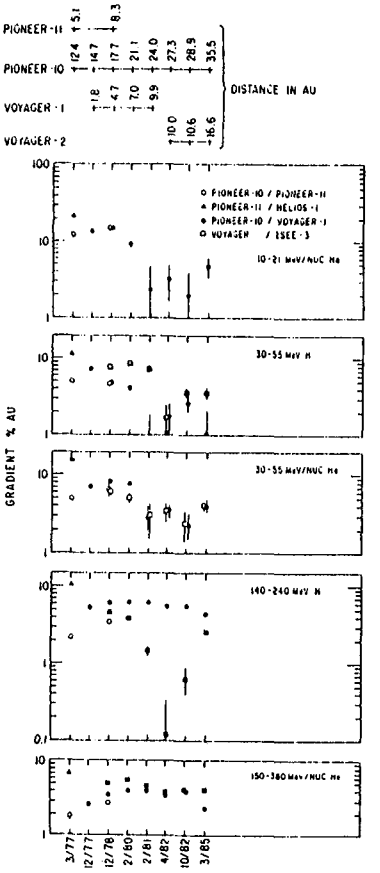

Fig 19

5.2.3 Latitudinal Gradient

The latitudinal gradient of galactic cosmic rays is considered in only one paper, SH4.7-6. Venkatesan *et al.* show that the upper limit on the latitudinal gradient of > 70 MeV protons between the Voyagers decreased from ~ 0.42 %/deg, to ~ 0.13 %/deg from early 1981 till late 1984. They also hold the view that no significant latitudinal gradient existed (Decker *et al.*, 1984).

5.2.4 Implications

A simple-minded interpretation of the gradient measurements does not seem possible. For example, Venkatesan interpret the decreasing trend of G_r to mean the approach of the modulation boundary (which would be reached when $G_r = 0$ %/AU).

In contrast, Fillius *et al.* estimate the location of the boundary by extrapolating the measured radially dependent intensity to intersect the estimated interstellar intensity. In this approach, a decreasing G_r implies that the modulation boundary is receding instead.

For more sophisticated considerations, the reader is referred to Kota (1985).

5.3 The Anomalous Component

Anomalously high quiet-time fluxes of He, N, O and Ne were first discovered in 1972 at < 30 MeV/nuc. They were observed in the solar minimum period 1972 - 1978 but have not been observed at 1 AU since 1979. Fisk *et al.* (1974) suggest that they are interstellar neutrals that, after entering the heliosphere, become singly ionised by solar UV or charge exchange and are subsequently accelerated in the interplanetary medium. Pesses *et al.* (1981) put forward a model in which these singly ionised particles are accelerated instead in the polar regions of the

solar wind termination shock, and then drift into the equatorial region of the heliosphere. This latter model predicts a 22-year modulation cycle dependent on the sign of the solar magnetic field, and that the anomalous component will not return in the coming solar minimum.

Recent observations of the intensities, radial and latitudinal gradients of the anomalous components have been closely monitored to see what light they may shed on their origin, acceleration and modulation.

5.3.1 Changes in the Intensity Spectrum of Anomalous O and He

Observations at 1 AU.

Various experimental data on anomalous O and/or He from IMP-8, ISEE-3/ICE and ISEE-1 have bee carefully analysed by Mewaldt and Stone (SH4.6-2), Mason *et al.* (SH4.6-3) and McKibben *et al.* (SH4.7-5). Their unanimous conclusion is that by end 1984/early 1985 anomalous O and He had shown no sign of recovery. However, Mewaldt and Stone as well as Mason *et al.* point out that since neutron-monitor rates had not returned to levels that imply observable anomalous O flux based on an 11-yr cycle, we probably have to wait for the next ICRC to know e.g. if Pesses *et al.*'s model applies.

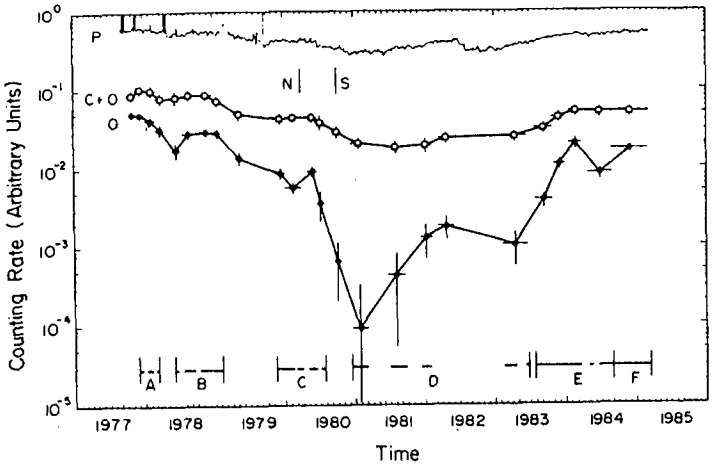

Fig 20

Observations in the Outer Heliosphere

By late 1984/early 1985, the intensity of anomalous He had not recovered at Voyagers 1, 2 and Pioneer 10 at ~16 AU, ~22 AU and ~32 AU respectively, as reported by Cummings *et al.* (SH4.6-1), McDonald *et al.* (SH4.7-3) and McKibben *et al.*(SH4.7-5). In contrast, anomalous O at Voyager 1 rose by a factor ~100 from its low level in 1981 (Fig 20, from paper SH4.6-4 by Webber *et al.*) This is consistent with anomalous O being singly ionised with rigidity ~2 GV.

Cummings *et al.* show that the anomalous O spectrum changed dramatically soon after solar field reversal in 1980 (Fig 21). They report that this is similar to the predicted spectral changes in a recent model of Jokipii (1985), which includes acceleration at solar wind termination shock and drifts.

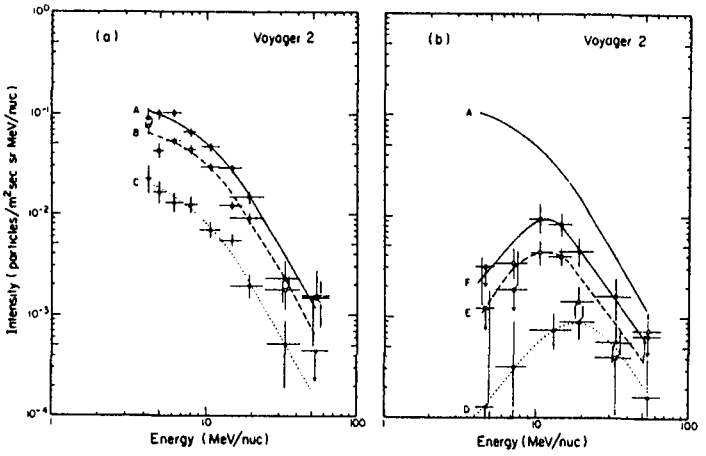

Fig 21

They also note that the observed absence of anomalous He below 30 MeV/nuc and the reduced intensity of anomalous O below 8 MeV/nuc in late 1984 are consistent if both species were singly ionised (see their Fig 4).

5.3.2 Radial and Latitudinal Gradients of the Anomalous O and He

Figure 22 from Webber *et al.* (SH4.6-4) show that the radial gradient of anomalous O as measured on Voyagers 1, 2 and Pioneer 10 in 1977 -1985 remains essentially constant at 10 - 15 %/AU although the intensity has varied by a factor of 100. They also report a latitudinal gradient of 3 ± 1 %/deg for anomalous O in the 7.1 - 10.6 MeV/nuc interval only, between Voyagers 1 and 2 at 15 - 20 AU from late 1983 to early 1985. In contrast, the radial gradient of 11 - 20 MeV/nuc He experienced a dramatic decrease in both the inner and outer heliosphere from ~10 %/AU before to 0 - 2 %/AU after the solar field reversl in 1980 (SH4.7-3 and 5, see also Figs 18 and 19).

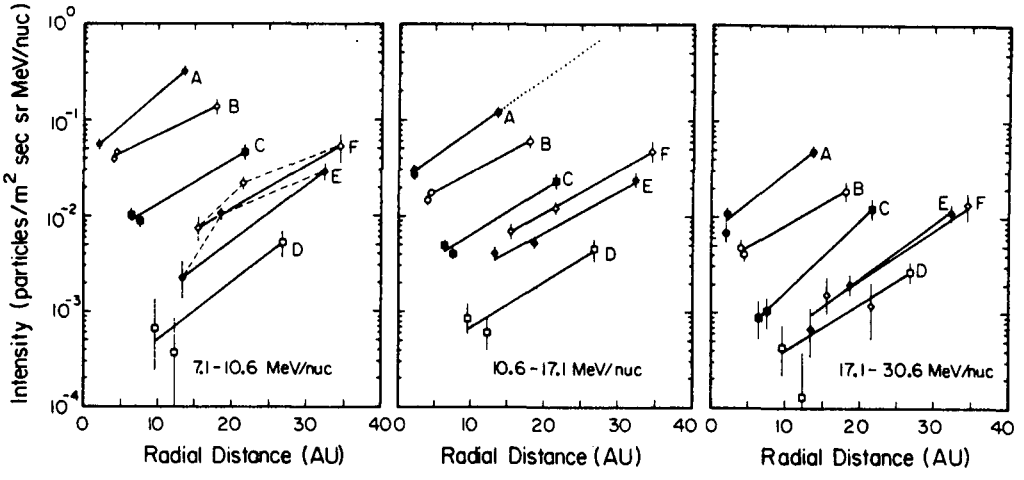

Fig 22

In terms of the conventional model of modulation, Webber *et al.* show that the intensity modulation between periods A and D in Fig 20 can be produced by a shift of 46 ± 4 AU in the modulation boundary. They further show that, if O is singly ionised, this boundary change also implies intensity modulation of a factor ~ 2 and G_r ~ 1.5 %/AU for relativistic particle of ~ 1.8 GV in rough agreement with other observations.

However, it is not clear that the conventional model can produce the spectral change of anomalous O discussed earlier. On the other hand, Pesses *et al.*'s model may have difficulty fitting the observed G_r (see section 5.3.4).

5.3.3 Origin

Observation of singly ionised He suggested to be ex-interstellar neutrals is reported for the first time by Hovestadt *et al.* (SH4.6-6). Figure 23 shows the energy spectrum of particles of M/Q = 4 measured by a time-of-flight spectrometer aboard the IRM spacecraft at 1 AU. The spectrum has a sharp cut-off at 23 KeV/Q, which for He^+ corresponds to a top speed of 2W, where W = solar wind speed. Freshly ionised helium should have a top speed of 2W sinα, where α is the angle between the solar wind flow and the magnetic field. Thus the observed cut-off energy, shown to correlate strongly with $(1/2)M(2W)^2$ rather than with $(1/2)M(2W \sin\alpha)^2$ in their Fig 3 and 4, indicate the particles have suffered substantial pitch-angle scattering since ionisation. Hovestadt *et al.* also use their observation to estimate an interstellar neutral helium density of ~ 0.01/cm³, compatible with other reported values. They suggest the observed particles to be neutral interstellar helium ionised by solar UV and that these represent the source of anomalous He as suggested by Fisk *et al.* (1974).

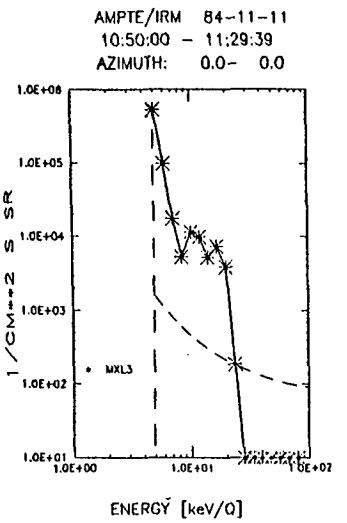

Fig 23

5.3.4 Theories

In paper SH4.6-7A, Biswas *et al.* propose that the anomolous component originates in the stellar winds of O-type stars located in a region a few Kpc around the solar system. They suggest that 10 - 100 KeV/nuc heavy ions of He^{+2}, O^{+4}, etc. in these hot stellar winds are further accelerated to 5 - 100 MeV/nuc at the shock fronts of supernova remnants, and then enter the solar system via interstellar magnetic field lines connected to the solar field. If this is correct, the anomalous component should suffer the same solar modulation as other galactic cosmic rays of comparable rigidities.

In paper SH4.6-6 Potgieter *et al.* study a model that includes gradient and curvature drifts, a diffusion coefficient appropriate for solar minimum, and a source located at various latitudes on a boundary at 50 AU. They show that for a source over the solar pole, irrespective of the IMF polarity, the radial gradient decreases very rapidly with radius

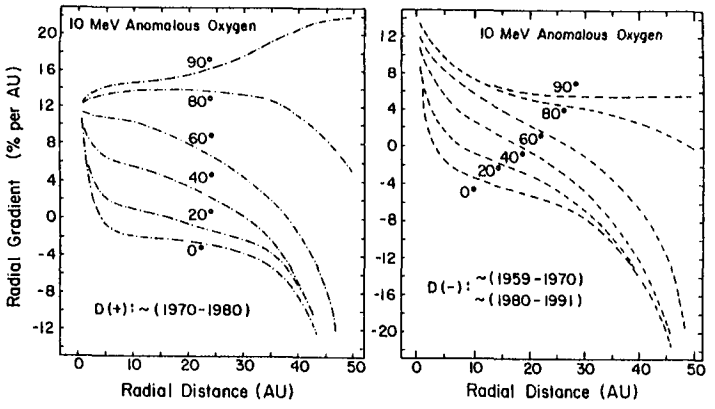

Fig 24

in the equatorial plane, from ~10 %/AU to negative values beyond ~ 5 AU (Fig 24), inconsistent with observed gradients of the anomalous O (see above). With a source located on the equator, acceptable positive gradients are produced but the predicted intensity dependence on the IMF polarity is inconsistent with observation at Earth. They conclude that models assuming termination-shock acceleration and drifts as in Pesses *et al.* (1981) cannot fit the observation. However, Jokipii claims that the predictions of his recent model with these features agree with both the spectral and gradient observations.

6. Concluding Remarks

The reports at the conference underscore the importance of

(a) analysing particle directional anisotropies in both GLEs and spacecraft observed events, in understanding pitch-angle scattering by magnetic turbulence and the focusing effect of the IMF

(b) having many observation posts ,i.e. spacecraft, to study coronal and interplanetary propagation

(c) correlative studies of multi-spacecraft particle data with solar electromagnetic emissions and synoptic maps of the coronal magnetic field, in deciding e.g. whether coronal diffusion or shock acceleration is operative far from the flare site

(d) drifts in particle acceleration by quasi-perpendicular shocks, and the inclusion of scattering in the SDA model

(e) the deep space network for studying long-term solar modulation and short-term modulation by shocks

(f) the future Ulysses mission in providing the much needed 3-D view of solar modulation.

The experimental determination of the rigidity dependence of the interplanetary mean free path below ~200 MeV is still controversial and more work needs to be done. In particular, the effect of the flare shock as a continuous moving particle source and a reflector should be

modelled.

The exact mechanism of solar modulation and the origin of the anomalous component remain controversial, although both drifts and cumulative shock modulation are recognised to be important. However, this is the subject of another rapporteur paper of this conference (Kota, 1985).

It is hoped that by the next ICRC, much progress would have been made and many of these controversies would be resolved.

Acknowledgements

I wish to thank many of the authors for stimulating and helpful discussions and to B.L. Ng for her patient typing of the manuscript.

References

Bazilevskaya, G.A. and E. V. Vashenyuk (1979) 16th ICRC, Kyoto, *5*, 156.
Burlaga, L. *et al.* (1983) Geophys. Res. Lett., *10*, 413.
Christon, S.P. and E.C. Stone (1985) Geophys. Res. Lett., *12*, 109.
Decker, R.B. (1983) J. Geophys. Res., *88*, 9959.
Decker, R.B. *et al.* (1984) Astrophys. J., *278*, L122.
Evenson, P. *et al.* (1983) Astrophys. J., *275*, L15.
Fisk, L.A. *et al.* (1974) Astrophys. J., *190*, L35.
Jokipii, J.R. (1982) Astrophys. J., *255*, 716.
Jokipii, J.R. (1985) Submitted to J. Geophys. Res.
Kota, J, (1985) 19th ICRC, San Diego, Rapporteur paper.
Lee, M.A. (1983) J. Geophys. Res.,*88*, 6109.
Lin, R. P. and H. S. Hudson (1976) Solar Phys., *50*, 153.
Lockwood, J.A. *et al.* (1982) J. Geophys. Res., *87*, 4338.
Mason, G.M. *et al.* (1984) Astrophys. J., *280*, 902.
McGuire, R. E. *et al.* (1983) 18th ICRC, Bangalore, *10*, 353.
Mullan, D.J. (1983) Astrophys. J., *269*, 765.
Mullan, D.J. and K.H. Schatten (1979) Solar Phys., *62*, 153.
Newkirk, G., Jr. and D.G. Wentzel (1978) J. Geophys. Res., *83*, 2009.
Ng, C.K. and L.J. Gleeson (1976) Solar Phys., *46*, 347.
Ng, C.K. *et al.* (1983) 18th ICRC, Bangalore, *10*, 381.
Pesses, M.E. *et al.* (1981) Astrophys. J., *246*, L85.
Reid, G.C. (1964) J. Geophys. Res., *69*, 2659.
Scholer, M. (1985) 19th ICRC, San Diego, Highlight talk.
Steinolfson, R.S. and D.J. Mullan (1980) Astrophys. J., *241*, 1186.
Van Hollebeke, M.A.I. (1979) Rev. Geophys. Space Phys., *17*, 545.
Webb, G.M. (1983) Astron. Astrophys., *124*, 163.